UCRL-10630 Rev.

c.2

University of California

Ernest O. Lawrence Radiation Laboratory

THE INFLUENCE OF HIGH PRESSURES ON THE MÖSSBAUER EFFECT IN DYSPROSIUM-161

Berkeley, California

DISCLAIMER

Submitted to Phys. Rev.

UCRL-10630-Rev.

UNIVERSITY OF CALIFORNIA

Lawrence Radiation Laboratory
Berkeley, California

Contract No. W-7405-eng-48

THE INFLUENCE OF HIGH PRESSURES ON THE MÖSSBAUER EFFECT IN DYSPROSIUM-161

J. A. Stone, M. Nicol, G. Jura, and J. O. Rasmussen

April, 1963

THE INFLUENCE OF HIGH PRESSURES ON THE MÖSSBAUER EFFECT IN DYSPROSIUM-161

J. A. Stone, M. Nicol, G. Jura, and J. O. Rasmussen

Lawrence Radiation Laboratory
and Department of Chemistry
University of California
Berkeley, California

April 1963

ABSTRACT

Nuclear resonance absorption of the 25.6-keV gamma ray of Dy^{161} has been studied experimentally at pressures up to 100 kbar by using sources situated in gadolinium metal together with thin metallic dysprosium absorbers. Velocity spectra taken at 30 and 50 kbar show complex hyperfine structure. Increasing the pressure leads to both greater recoil-free fractions and greater overall hyperfine splitting. The effect of pressure on the recoil-free fraction is satisfactorily explained with a modification of Hanks' theoretical treatment. It is proposed that the hyperfine splitting is predominantly due to electric quadrupole interactions, with the electric field gradient at the nucleus increasing with increasing pressure. By fitting theoretical spectra to the velocity spectrum at 30 kbar, a value of 1.30 is derived for the ratio of the quadrupole moments of the 25.6-keV state and the ground state of Dy^{161}.

THE INFLUENCE OF HIGH PRESSURES ON THE MÖSSBAUER EFFECT IN DYSPROSIUM-161*

J. A. Stone†, M. Nicol, G. Jura, and J. O. Rasmussen

Lawrence Radiation Laboratory
and Department of Chemistry
University of California
Berkeley, California

April 1963

I. INTRODUCTION

The pressure dependence of the Mössbauer effect has been treated theoretically by Hanks.[1] High pressures are expected to cause an enhancement of recoil-free fractions, in a manner similar to that of low temperatures, by the creation of a more rigid crystalline lattice. No experimental information has been available to confirm this theoretical conclusion, although Pound et al.[2] performed experiments with Fe^{57} at pressures up to 3 kbar, in which line shifts were sought. The present paper deals with the results of experiments at pressures up to 100 kbar with the 25.6-keV gamma ray of Dy^{161}. The emitting and absorbing nuclei were embedded in gadolinium and dysprosium metals, respectively. With this system a pressure dependence is found for both the recoil-free fraction and the hyperfine splitting.

Nuclear resonance absorption has been previously observed with Dy^{161} by Ofer et al.[3,4] These workers studied the resonance effect in several crystalline environments at room temperature and at lower temperatures. More recent work by a group at Manchester[5,6] gives the temperature dependence of the hyperfine structure (hfs) for a metallic Dy absorber in its antiferromagnetic state (85 to 175°K). An interesting result of their work is that large hyperfine splittings are observed from magnetic interactions, but that these

splittings disappear with the transition to the paramagnetic state at the Néel point. (A similar phenomenon has been observed with Fe^{57} in iron metal;[7] the hfs pattern collapses into a single line at the Curie point.)

For the present work it is necessary to extend the theory of Hanks to the case in which the ambient temperature T is greater than the Debye temperature θ for the emitting atoms. The recoil-free fraction f is given by a Debye-Waller factor,

$$\ln f = -\frac{3R}{2k\theta}\left[1 + 4\left(\frac{T}{\theta}\right)^2 \int_0^{\theta/T} \frac{t\,dt}{e^t - 1}\right], \qquad (1)$$

where R is the recoil energy of an atom upon emission of a gamma ray, and k is Boltzmann's constant. For the case where $T/\theta \gg 1$, one may proceed in the following manner. When T/θ is greater than about 1.6, the integral in Eq. (1) is well approximated by[8]

$$4\left(\frac{T}{\theta}\right)^2 \int_0^{\theta/T} \frac{t\,dt}{e^t - 1} \approx 4\left(\frac{T}{\theta}\right) - 1 . \qquad (2)$$

This yields a very simple high-temperature expression for the recoil-free fraction:

$$\ln f = -\frac{6RT}{k\theta^2}, \qquad (T/\theta > 1.6). \qquad (3)$$

It is convenienct to work with the ratio f_2/f_1 of recoil-free fractions at pressures P_2 and P_1, given by

$$\ln \frac{f_2}{f_1} = -\frac{6RT}{k}\left(\frac{1}{\theta_2^2} - \frac{1}{\theta_1^2}\right). \qquad (4)$$

Hanks obtains the volume dependence of θ from the Grüneisen relation, and, by assuming small volume changes, he gives the following expression:

$$\left(\frac{1}{\theta_2}\right)^2 \approx \left(1 - 2\gamma \frac{\Delta V}{V_1}\right)\left(\frac{1}{\theta_1}\right)^2 . \qquad (5)$$

Here γ is the Grüneisen constant for the material, and $\Delta V/V_1 = (V_1-V_2)/V_1$. This may be inserted into Eq. (4) to give

$$\ln \frac{f_2}{f_1} = \frac{12\ RT\gamma}{k\theta_1^2} \frac{\Delta V}{V_1} . \qquad (6)$$

For convenience the ratio f_2/f_1 at arbitrary pressures P_2 and P_1 may be expressed in terms of quantities at the reference pressure P_o = 1 atm by

$$\ln \frac{f_2}{f_1} = \frac{12\ RT\gamma}{k\theta_o^2}\left(\frac{V_o-V_2}{V_o} - \frac{V_o-V_1}{V_o}\right) = \frac{12\ RT\gamma}{k\theta_o^2}\left(\frac{\Delta V_2}{V_o} - \frac{\Delta V_1}{V_o}\right). \qquad (7)$$

This expression is general for the case of $T/\theta \gg 1$. Later it will be simplified even further by use of the conditions which held during the experimental work described herein.

II. EXPERIMENTAL METHODS

A. Materials Preparation

Sources in the form of Gd metal discs containing radioactive Tb^{161} were used throughout this work. Discs were machined from a large piece of commercially-obtained Gd metal of natural isotopic composition. To meet the requirements of the high-pressure apparatus, each disc was 3/16 in. in diameter and 0.0070±0.0005 in. thick. Neutron irradiation of these machined samples produced the $Gd^{160}(n,\gamma)Gd^{161}$ reaction, followed by the beta-decay of 3.7-min Gd^{161} to 7-day Tb^{161}. Sources prepared in this manner were used directly in the experiments, without the necessity of further chemical or metallurgical procedures.

Absorbers prepared by vacuum evaporation of natural Dy metal onto an aluminum backing foil were used. The average thickness of each foil was 10 mg/cm^2 of Dy.

B. Production of High Pressures

Pressure was transmitted to a source disc by means of anvils of the type developed by Bridgman,[9] with the design modifications described by Harris et al.[10] They are shown in Fig. 1. Each anvil is tapered with an angle of 5 deg, except for the $\frac{1}{4}$-in. flat portion at the center. Between the flat portions of two anvils are contained the sample and a gasket in the form of a ferric-oxide-coated pyrophyllite ring. A detailed view of this pressure chamber is shown in Fig. 2. Pressure was applied to the anvil assembly by a hydraulic press with 100-ton capacity.

The loading pressure on the ram of the press could be accurately measured, although this quantity is not necessarily an accurate measure of the true pressure on the sample. With Bridgman-type anvils Montgomery et al.,[11]

found that a radial pressure gradient existed in the sample, with the pressure at the center of a sample of silver chloride somewhat lower than the pressure at its edge. However, at constant radius they found that the true pressure is proportional to the loading pressure.

C. Gamma-Ray Spectroscopy

The velocity spectrometer used in this work is a constant velocity device that utilizes a rotating-disc absorber. It is similar to the apparatus described by Shirley et al.,[12] in which the absorber is driven by a synchronous motor and an audio oscillator.

Gamma rays were detected by a standard NaI scintillation counter. The counting geometry required for the high-pressure experiments was quite poor. As shown in Fig. 2, only those gamma rays that escape from the edge of the source disc can be detected. The half-thickness of Gd metal for photoelectric absorption of 25.6-keV gamma rays is estimated to be only 0.05 mm, so that virtually all the photons that reach the detector are emitted from a very small volume at the edge of the sample. This is important because the effects of the radial pressure gradient in the source are then minimized. Since most of the photons that escape arise within a distance which is a very small fraction of the radius of the sample, the variation of pressure over this distance is also quite small.

III. RESULTS

A. Introduction

The earliest work in this research was largely exploratory in nature. Short experiments were performed at a number of pressures between one atmosphere and 30 kbar in an effort to determine quickly whether large absorption effects would occur in this system in this pressure range. Although these experiments were by no means sufficiently thorough to give detailed velocity spectra, below 25 kbar no large absorption effects were observed. However, at a pressure near 30 kbar, qualitative evidence for several deep resonance minima was obtained. It was at this pressure, therefore, that a thorough systematic study of the velocity spectrum was made. Later a similar study was performed at a pressure near 50 kbar. Finally, an effort was made to obtain the velocity spectrum at a pressure near 100 kbar, as well as to repeat the experiment at atmospheric pressure with greater precision. The results of these experiments will be given in the following sections.

For convenience, the three principal elevated pressures that were used will be labelled 30 kbar, 50 kbar, and 100 kbar. As discussed in Sec.II-B, an exact knowledge of absolute pressures was not available, so that the above numbers are merely useful for the identification of different experiments. However, the nominal pressures of the experiments, as calculated from the loadings lie very near these numbers, so that the general regions of pressure are correctly indicated.

From a velocity spectrum it is possible to extract a quantitative value for the relative recoil-free fraction. Shirley et al.[12] have shown that the recoil-free fraction f is directly proportional to the area above a transmission curve, and that the proportionality constant depends only upon

parameters related to the absorber. Therefore, for two experiments that use the same absorber,

$$\frac{f_2}{f_1} = \frac{(\text{Area})_2}{(\text{Area})_1} = \frac{\int_{-\infty}^{+\infty} \left[1 - T_2(v)\right] \, dv}{\int_{-\infty}^{+\infty} \left[1 - T_1(v)\right] \, dv} , \qquad (8)$$

where $T(v)$ is the transmitted intensity of gamma rays at velocity v, normalized to the transmitted intensity at a velocity far off resonance. Thus, without explicit knowledge of the absorber parameters, a ratio of recoil-free fractions may be obtained. In the following sections use is made of this relationship to give the recoil-free fraction at a pressure P relative to that at 30 kbar. The trend of the quantities f_P/f_{30} will be adequate to define the pressure dependence of the recoil-free fraction.

The overall width of a velocity spectrum will be treated in the following manner to obtain quantities related to the overall width of the emission pattern. A quantity ΔE is defined as the energy difference between the highest- and lowest-energy component of the emission hfs pattern, i.e., the overall width for the source. Similarly, a quantity ΔE_a is defined for the absorber. Then, the observed width of a velocity spectrum ΔE_{obs} is the sum of ΔE and ΔE_a. For two experiments using the same absorber an expression independent of ΔE_a is given by

$$\Delta E_2 - \Delta E_1 = (\Delta E_{obs})_2 - (\Delta E_{obs})_1 . \qquad (9)$$

The quantities ΔE_{obs} and $\Delta E_P - \Delta E_{30}$ will be given at each pressure.

In the cases for which it was possible to do so, the velocity coordinate of the spectrum centroid was computed. This is given by

$$\bar{v} = \frac{\int_{-\infty}^{+\infty} \left[1 - T(v)\right] v \, dv}{\int_{-\infty}^{+\infty} \left[1 - T(v)\right] dv} \quad . \tag{10}$$

The quantity $\bar{v}$ is of interest as a measure of the chemical shift between Dy^{161} in Gd and Dy^{161} in Dy.

B. Velocity Spectrum at 30 kbar

The transmission spectrum as a function of relative velocity for the 30 kbar experiment is shown in Fig. 3. The curve is defined by approximately 100 data points taken at velocity increments of 0.37 mm/sec, with an average statistical error per point of ±0.26%. Each portion of the spectrum was measured at least four times, with different sources, over a period of about one year. Reproducibility of all the features of this spectrum was excellent. These data were taken at a loading of 3500 psi, corresponding to a nominal pressure of 30.8 kbar.

Two features of this spectrum are readily apparent. First, there is a complex hfs; and, secondly, the pattern is asymmetric, both with respect to zero velocity and with respect to the line positions. A measure of the asymmetry about zero velocity is given by the velocity coordinate of the centroid: $\bar{v} = 4.0 \pm 0.2$ mm/sec. An interpretation of the asymmetric hfs will be given in Sec. IV-B.

As mentioned earlier, this spectrum will serve as a reference for the description of the spectra at other pressures. For this reason, considerable

effort was spent in reducing the statistical error of the points and in accurately defining the line positions. The area above the curve and the overall width of the spectrum have been used to obtain the values of f_P/f_{30} and $\Delta E_P - \Delta E_{30}$ reported in the following sections.

C. Velocity Spectrum at 50 kbar

The transmission spectrum for the experiment at 50 kbar is shown in Fig. 4. The curve is defined by approximately 200 data points taken at velocity increments of 0.37 mm/sec, with an average statistical error per point of ±0.4%. Each portion of the spectrum was measured at least twice, with different sources, over a period of about six months. Most of the features of this spectrum were reproducible, although certain portions were repeated several times because of poor reproducibility. These data were taken at a loading of 6000 psi, corresponding to a nominal pressure of 52.8 kbar.

It should be noted that the hfs of the 50 kbar spectrum is even more complex than that of the 30 kbar spectrum. There appear to be approximately twice as many lines in the 50 kbar spectrum, spread over a larger velocity range. Again the pattern is asymmetric about zero velocity, as indicated by the velocity coordinate of the centroid: $\bar{v}$ = 2.0±0.4 mm/sec. From the area above the curve one obtains f_{50}/f_{30} = 1.81±0.05. The overall width of the transmission curve compared with the 30 kbar spectrum is given by $\Delta E_{50} - \Delta E_{30}$ = 2.67±0.05 cm/sec.

D. Results at Other Pressures

An experiment at atmospheric pressure was performed by using a loud-speaker-driven velocity spectrometer.[13] The use of this device permitted a much larger counting geometry than was possible in the high-pressure experiments. Also, the continuously varying velocity eliminated the need for source-decay corrections. The velocity scale for the experiment was established by a measurement of the well-known velocity spectrum of Fe^{57} in Fe metal.[14] With Dy^{161}, counts were taken repeatedly until a statistical accuracy of better than 0.1% for each velocity point was attained. The results of this experiment were negative: no nuclear resonance absorption effects were found within the statistical accuracy quoted. Consequently, it is possible to set an upper limit on the recoil-free fraction at 1 atm relative to that 30 kbar as $f_0/f_{30} \lesssim 0.3$.

Finally, an experiment was performed at a loading of 11,000 psi, corresponding to a nominal pressure of 96.7 kbar. This pressure, previously referred to as 100 kbar, was considered to be about the practical upper limit for a counting experiment with the existing equipment. Even though a considerable amount of data was taken at this pressure, the results are complicated by several experimental difficulties. Nevertheless, some useful information could be obtained from the data. In particular, the overall width of the spectrum was easily measured to give $\Delta E_{100} - \Delta E_{30} = 5.5 \pm 0.2$ cm/sec. The relative recoil-free fraction could be obtained, with a very large error; the result is $f_{100}/f_{30} = 3 \pm 1$. There was some evidence for hfs throughout the spectrum, but the large error prevents giving a detailed velocity spectrum.

E. Summary and Comparison of Results

The quantitative results of the previous sections are brought together for comparison in Table I. In Fig. 5 the general shapes of the velocity spectra are compared schematically. The curves in Fig. 5 represent smoothed velocity spectra arbitrarily drawn through the data points. A smoothed velocity spectrum may be thought of as a smooth curve upon which the hfs is to be superimposed to give the experimental spectrum. Smoothed velocity spectra are used here for the graphical comparison of widths, areas, and shapes to avoid the added complexity of hfs. Indeed, for the 100-kbar spectrum only the smoothed velocity spectrum can be given from the data, and this with considerably less accuracy than for the other two curves in Fig. 5.

Two qualitative conclusions may be drawn immediately from this comparison. With increasing pressure:

(1) recoil-free fractions increase;

(2) hyperfine splittings increase.

These two effects summarize the influence of high pressures on the Mössbauer effect in Dy^{161} as determined from this experimental work. The interpretation of these results will be discussed in the following sections.

IV. DISCUSSION

A. Recoil-Free Fractions

Equation (7) may be placed in a form more suitable for comparison with the experimental results by introduction of the Slater expression[15] for the pressure dependence of $\Delta V/V_o$,

$$\frac{\Delta V}{V_o} = aP - bP^2, \qquad (11)$$

where a and b are here considered as empirical parameters. In addition, use

is made of the proportionality between pressure and loading to define a new variable, x:

$$\frac{P_2}{P_1} = \frac{L_2}{L_1} = x. \qquad (12)$$

By using a ratio of accurately known loadings the uncertainties in the pressure scale are avoided. With some rearrangement the final result is

$$\ln \frac{f_2}{f_1} = \frac{12\, RT\gamma}{k\theta_o^2} \left(\frac{\Delta V_1}{V_o} - bP_1^2 x \right) (x - 1). \qquad (13)$$

After inserting the value of the recoil energy for the 25.6-keV gamma transition in Dy^{161}, and, from the work of Bridgman,[16] volume data for the 30-kbar reference state, an expression is obtained that is suitable for comparison with the experimental results. Debye temperatures for pure Dy and Gd metals, as obtained from heat capacity measurements,[17] are near the value 150°K; however, the appropriate Debye temperature for a Dy impurity in Gd metal is not known. Values for the Grüneisen constants of these metals are available,[18] but the results of two different methods of obtaining the constants do not agree. Therefore, Eq. (13) is fitted to the high-pressure data points by considering θ_o^2/γ as an adjustable parameter.

With normal values of θ_o and γ one might expect to fit the experimental points with θ_o^2/γ of the order of 20,000. However, the data are actually fitted well with values of θ_o^2/γ of only 3600 to 6000. In Fig. 6 the four experimental points are shown together with the calculated curve for $\theta_o^2/\gamma = 6000$. An interpretation of this low value that appears the most reasonable and that is consistent with all the experimental data postulates that θ_o for the Dy impurity atom lies in the range 75° to 100°K. From Eq. (1) these values of θ_o correspond to recoil-free fractions of only 0.0003 to 0.01 at a pressure of one atmosphere. Thus, it is not surprising that no resonant absorption effects could be detected in the atmospheric-pressure experiment. The

magnitude of the Debye temperatures thus obtained agrees well with the picture of the impurity atom being less tightly bound in the lattice than are the host atoms.

Quantitative agreement is, therefore, obtained between the experimental results and the theory by making a reasonable assumption about the value of the Debye temperature of the impurity atom. Although Eq. (13) was derived with the help of some rather severe approximations, it nevertheless gives results that are apparently consistent with experiment. In particular, it satisfactorily explains the observed increase in recoil-free fractions with pressure.

B. Hyperfine Splittings

Due to the complexity of the velocity spectra, it is possible to give a detailed interpretation of only the 30-kbar data, where there is the greatest definition and the least number of lines. By using an IBM-7090 computer to generate the theoretical Mössbauer patterns, a successful fit to the velocity spectrum at 30 kbar was achieved using a simple model for the splitting mechanism. The essential features of this model are, first, that the emission line splitting is due entirely to electric quadrupole interactions in the source, and, secondly, that the absorber cross-section pattern consists of a narrow partially-resolved doublet. With these assumptions the most important adjustable parameter in the calculation becomes the ratio ρ of the quadrupole moment of the excited state to that of the ground state. A theoretical Mössbauer absorption pattern for $\rho = 1.30$ is shown in Fig. 7, together with the data points at 30 kbar. Small changes in ρ do not change the fit significantly, so that for the 26-keV state of Dy^{161}:

$$\rho = Q(26\text{-keV})/Q(\text{g.s}) = 1.30 \pm 0.05.$$

In Fig. 8 are shown the hyperfine gamma-ray components between two nuclear levels, each with I = 5/2, split by a pure electric quadrupole interaction.

Since both the sources and the absorber were in the paramagnetic state during these experiments, the assumptions used in deriving ρ, although imperfect, are reasonable. Previous work[5,7] with Fe^{57} and Dy^{161} shows that splitting due to magnetic interactions becomes very small when the emitting nuclei are in a paramagnetic host lattice. The value of ρ thus obtained may be compared with the ratio of quadrupole moments for the ground states of Dy^{163} and Dy^{161}. Both the ground state of Dy^{163} and the 25.6-keV state of Dy^{161} have the Nilsson quantum numbers[19] 5/2 - (523). In paramagnetic resonance measurements Park[20] found the ratio

$$Q(163)/Q(161) = 1.18 \pm 0.15,$$

which agrees with the present result. It should be noted that Boyle et al.[6] in their work with Dy^{161} interpreted deviations from a pure magnetic splitting pattern by quadrupole interactions with $\rho = 1$. In Fig. 8 are shown the splitting patterns for pure quadrupole interactions with $\rho = 1.00$ and $\rho = 1.30$. The symmetrical pattern results when $\rho = 1.00$, in contrast to the asymmetrical patterns observed in this experimental work.

At first glance it seems reasonable that the ratio of quadrupole moments for the odd-neutron in different spectroscopic states in Dy^{161} may differ from unity, but if we consider in detail the theoretical problem of equilibrium deformations of nuclei, it is not clear that such a difference in intrinsic quadrupole moments Q_o should be obtained here. Examination of the Nilsson diagram (Fig. 4 of Ref. 19) shows that the 5/2+ orbital (ground state of Dy^{161}) is more steeply down-sloping (energy decreasing with deformation) than the 5/2- orbital. We can easily make the qualitative prediction for nuclei with fewer neutrons than Dy^{161} that the odd nucleon

in the 5/2+ state should have a polarizing effect giving a greater deformation than in the 5/2- state. For nuclei with more neutrons than Dy^{161}, the reverse should be true, since the states are really "hole" states. For Dy^{161} itself the difference in deformation should probably be small, and it would require a detailed study including pairing forces to determine even the sense of the deviation from unity of the quadrupole ratio. Since it seems unlikely that the intrinsic quadrupole moments Q_o can vary so much between states our attention is drawn to the projection factor relating Q_{spec}, which we measure, and Q_o, the intrinsic moment.

$$Q_{spec} = \frac{3K^2 - I(I+1)}{(I+1)(2I+3)} Q_o$$

where I is the nuclear spin and K is the projection of the spin along the nuclear symmetry axis. Since the spins of ground and excited states are the same (I = 5/2), one would normally expect the same projection factor, for there should be a K of 5/2 in both cases. It is apparent that if K is not a good quantum number, and a spin 5/2 state possesses admixture of K = 3/2 and K = 1/2 components there will be a reduction in the observed Q_{spec}. The Dy^{161} ground band exhibits an anomalously close spacing that suggests a fair amount of mixing with the 3/2+ (651) band. To explain our quadrupole moment ratio of 1.3 assuming Q_o to be the same in ground and excited states, would require about 20% admixture of K = 3/2, or 13% of K = 1/2, or some combination of both. Such admixtures seem unduly large, but it is clear that the ground band of Dy^{161} deserves special attention with respect to breakdown of the K-quantum number.

If the viewpoint is taken that the overall splitting is predominantly due to the electric quadrupole interaction at all pressures up to 100 kbar, an interesting correlation may be obtained between the measured values of ΔE

and the quadrupole coupling constants B. For this purpose it is assumed that in the first approximation the relative energies of the sublevels are given by

$$E = (1/4)\, e^2qQ\, \frac{3m^2 - I(I+1)}{I(2I-1)}\,, \qquad (14)$$

where $B = (1/4)\, e^2qQ$. For both the 25.6-keV level and the ground state of Dy^{161}, this expression becomes

$$E = (0.3\, m^2 - 0.875)B \qquad (15)$$

By using Eq. (15), the relative energies of the seven gamma transitions between sublevels of the two states may be calculated as a function of ρ.

Since the quantity ΔE is defined as the energy difference between the highest- and lowest-energy gamma components, it may be obtained from the energy expressions. Due to crossovers in the energies as ρ is varied there are several ranges, each with a different expression for ΔE:

$$\Delta E = \begin{cases} (-1.8\ \rho + 1.8)\ B, & \rho \leq 0, \\ 1.8\ B, & 0 \leq \rho \leq 0.5, \\ (1.2\ \rho + 1.2)\ B, & 0.5 \leq \rho \leq 2, \\ 1.8\ \rho\ B, & 2 \leq \rho. \end{cases} \qquad (16)$$

A useful property of Eq. (16) is that no value of ρ gives a coefficient of B smaller than 1.8. Thus, when $\Delta E = 1.8\ B$, the values of B are absolute upper limits. Quadrupole coupling constants corresponding to $\Delta E \approx \Delta E_{obs}$ are given in Table II for both the upper limit and for $\rho = 1.30$, assuming that $\Delta E \gg \Delta E_a$.

A possible explanation for the increase in ΔE with pressure is that the energy bands in the rare earth metal, formed from 5d orbitals, cross the Fermi level at some pressure below 30 kbar. Then, if these 5d bands with different azimuthal quantum numbers are anisotropically populated, an

appreciable electric field gradient q at the nucleus may be produced. Also, if the 5d bands continue to decrease in energy with increasing pressure, an increasing electric field gradient will be produced, leading to increased splitting in accordance with the observed trend. It is interesting to note that the electric field gradient calculated for a single 5d electron on a Dy^{+3} ion gives quadrupole coupling constants of the same order as those obtained at 30 kbar. The same mechanism may be invoked using the energy bands formed from 6p orbitals; however, this is considered less likely because calculations by Rajnak[21] indicate that in the free ion the 6p state is considerably higher in energy than the 5d state.

FOOTNOTES AND REFERENCES

* Work done under the auspices of the U. S. Atomic Energy Commission.

† Present address: E. I. du Pont de Nemours and Company, Savannah River Laboratory, Aiken, South Carolina.

---

1. R. V. Hanks, Phys. Rev. 124, 1319 (1961).
2. R. V. Pound, G. B. Benedek, and R. Drever, Phys. Rev. Letters 7, 405 (1961).
3. S. Ofer, P. Avivi, R. Bauminger, A. Marinov, and S. G. Cohen, Phys. Rev. 120, 406 (1960).
4. R. Bauminger, S. G. Cohen, A. Marinov, and S. Ofer, Phys. Rev. Letters 6, 467 (1961).
5. A. J. F. Boyle, D. St. P. Bunbury, C. Edwards, and H. E. Hall, in Proc. Mössbauer Conf., 2nd, ed. by D. M. J. Compton and A. H. Schoen (John Wiley and Sons, New York, 1962), p. 182.
6. A. J. F. Boyle and H. E. Hall, Rept. Progr. Phys. 25, 441 (1962).
7. R. S. Preston, S. S. Hanna, and J. Heberle, Phys. Rev. 128, 2207 (1962).
8. F. C. Blake, Rev. Mod. Phys. 5, 169 (1933).
9. P. W. Bridgman, Proc. Am. Acad. Arts Sci. 81, 169 (1952).
10. R. E. Harris, R. J. Vaisnys, H. Stromberg, and G. Jura, in Progress in Very High Pressure Research, ed. by F. P. Bundy, W. R. Hibbard, Jr., and H. M. Strong (John Wiley and Sons, New York, 1960), p. 165.
11. P. W. Montgomery, H. Stromberg, G. H. Jura, and G. Jura, Lawrence Radiation Laboratory Report UCRL-9807, August 1961; ASME Pub. 62-WA-308.
12. D. A. Shirley, M. Kaplan, and P. Axel, Phys. Rev. 123, 816 (1961).
13. D. A. Shirley, M. Kaplan, R. W. Grant, and D. A. Keller, Phys. Rev. 127, 2097 (1962).

14. S. S. Hanna, J. Heberle, C. Littlejohn, G. J. Perlow, R. S. Preston, and D. H. Vincent, Phys. Rev. Letters 4, 177 (1960).

15. J. C. Slater, Phys. Rev. 57, 744 (1940).

16. P. W. Bridgman, Proc. Am. Acad. Arts Sci. 83, 1 (1954).

17. R. C. Skochdopole, M. Griffel, and F. H. Spedding, J. Chem. Phys. 23, 2258 (1955).

18. F. Barson, S. Legvold, and F. H. Spedding, Phys. Rev. 105, 418 (1957).

19. B. R. Mottelson and S. G. Nilsson, Kgl. Danske Videnskab. Selskab, Mat.-Fys. Skrifter 1, No. 8 (1959).

20. J. G. Park, Proc. Roy. Soc. (London) A245, 118 (1958).

21. K. Rajnak, J. Chem. Phys. 37, 2440 (1962).

Table I. Quantities measured in high-pressure Mössbauer-absorption experiments

P (kbar)	x	$\frac{f_P}{f_{30}}$	ΔE_{obs} (cm/sec)	$\Delta E_P - \Delta E_{30}$ (cm/sec)	$\bar{v}$ (mm/sec)
0 (1 atm)	~ 0	$\leqslant 0.3$	- -	- -	- -
30	1.00	1	3.15	0	4.0 ± 0.2
50	1.71	1.81 ± 0.05	5.82	2.67 ± 0.05	2.0 ± 0.4
100	3.14	3 ± 1	8.6	5.5 ± 0.2	- -

Table II. Quadrupole coupling constants derived from experimental splittings

Pressure (kbar)	B (Mc) Upper Limit	B (Mc) $\rho = 1.30$
30	360	235
50	670	435
100	1000	650

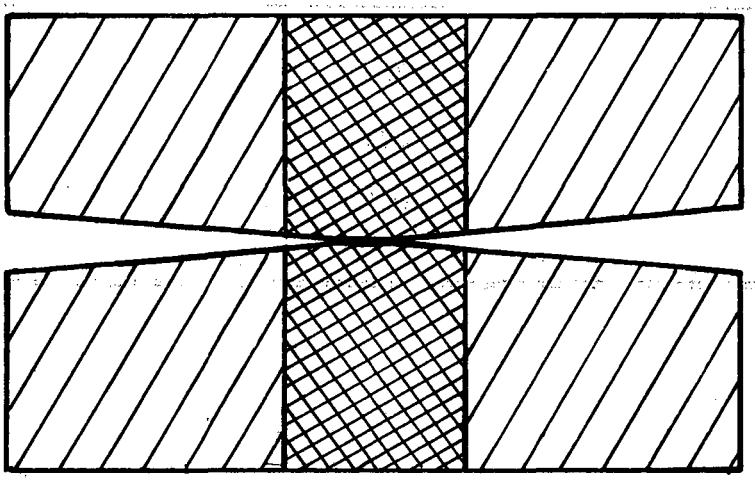

MU-29231

Fig. 1. Cross section of Bridgman-type anvils.

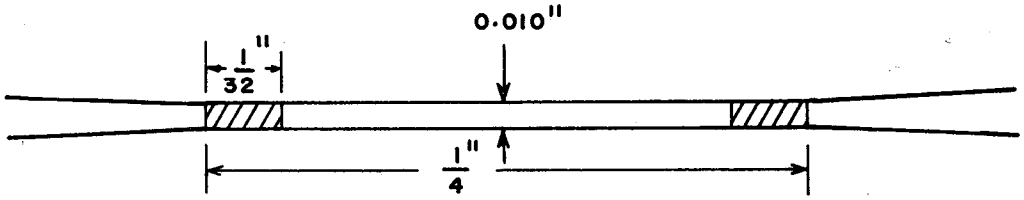

MU-29232

Fig. 2. Cross section of the pressure chamber between the faces of Bridgman-type anvils. The shaded areas are a pyrophyllite ring.

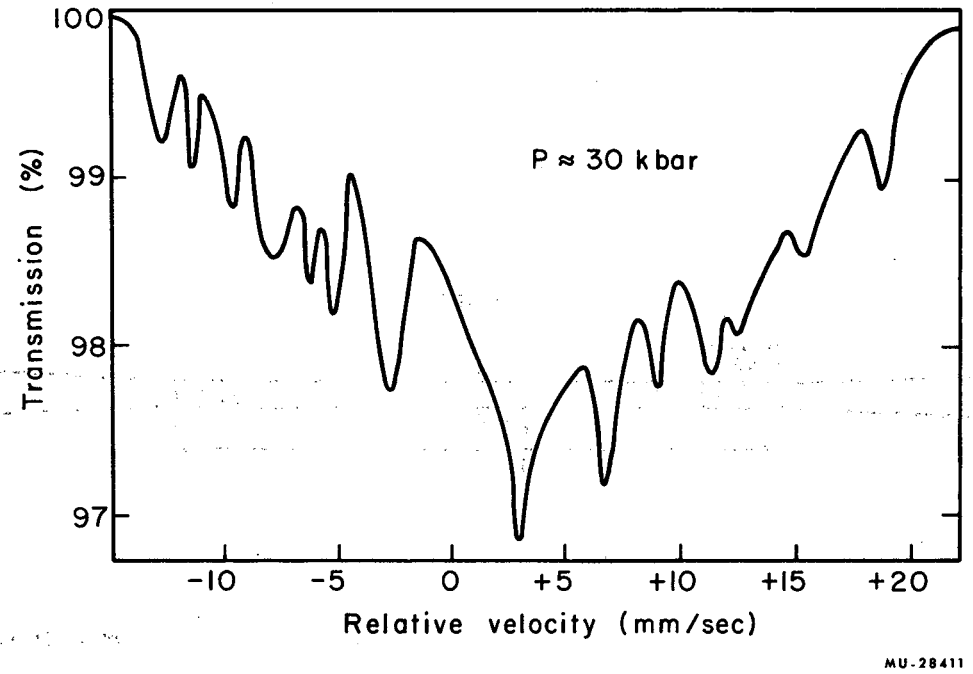

Fig. 3. Velocity spectrum at 30 kbar for Dy^{161} situated in Gd with a thin Dy absorber.

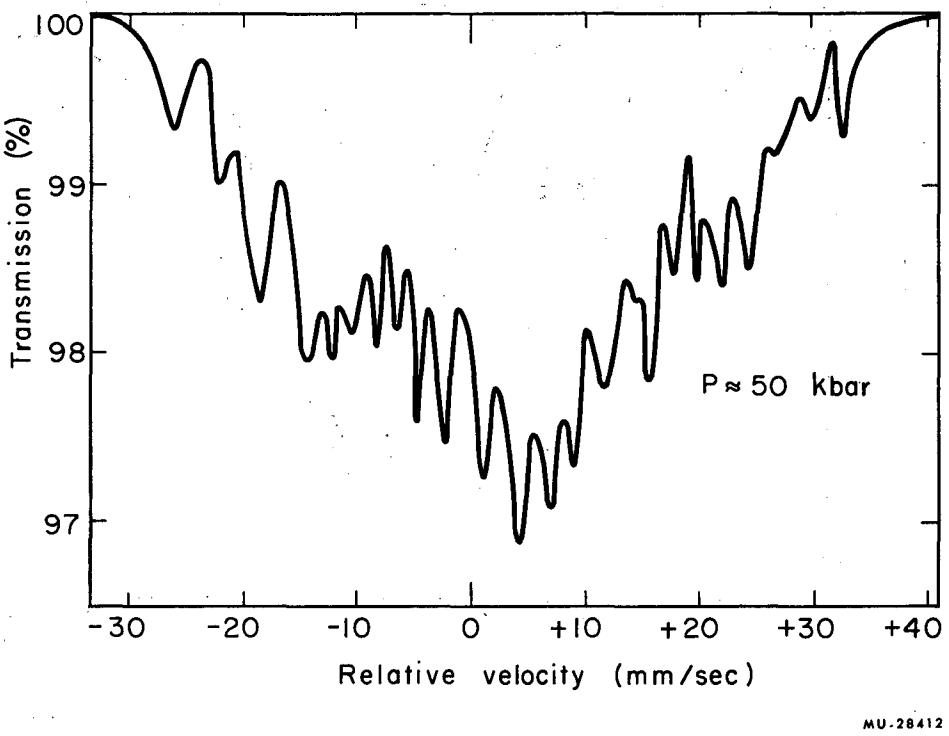

Fig. 4. Velocity spectrum at 50 kbar for Dy^{161} situated in Gd with a thin Dy absorber.

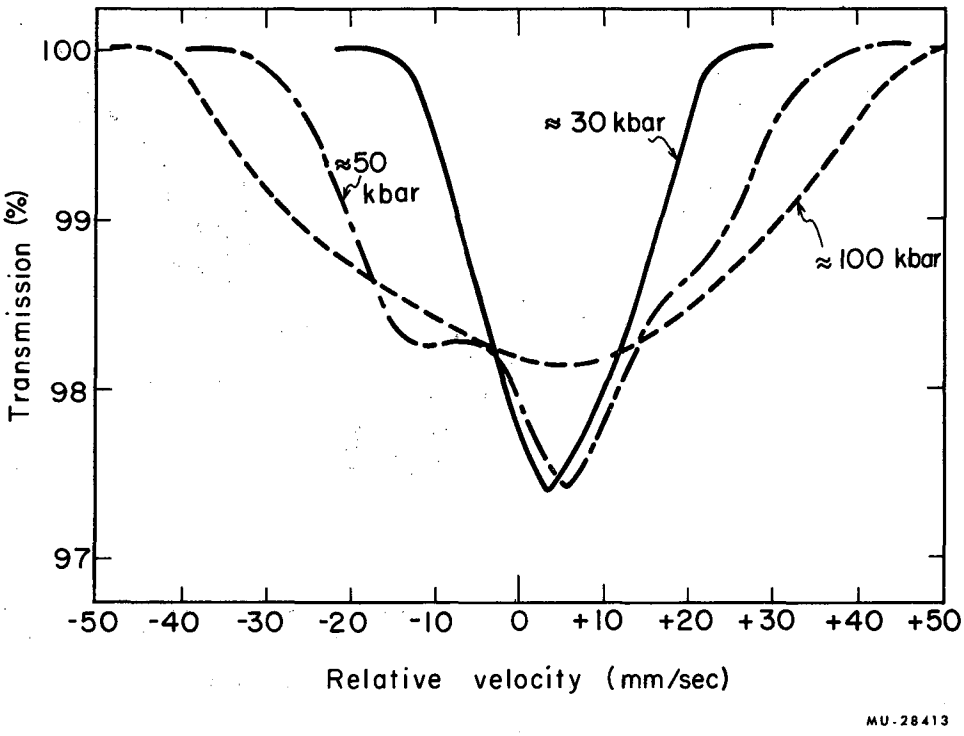

Fig. 5. Comparison of velocity spectra at several pressures for Dy^{161} situated in Gd with a thin Dy absorber. Hyperfine structure has been smoothed out of each curve.

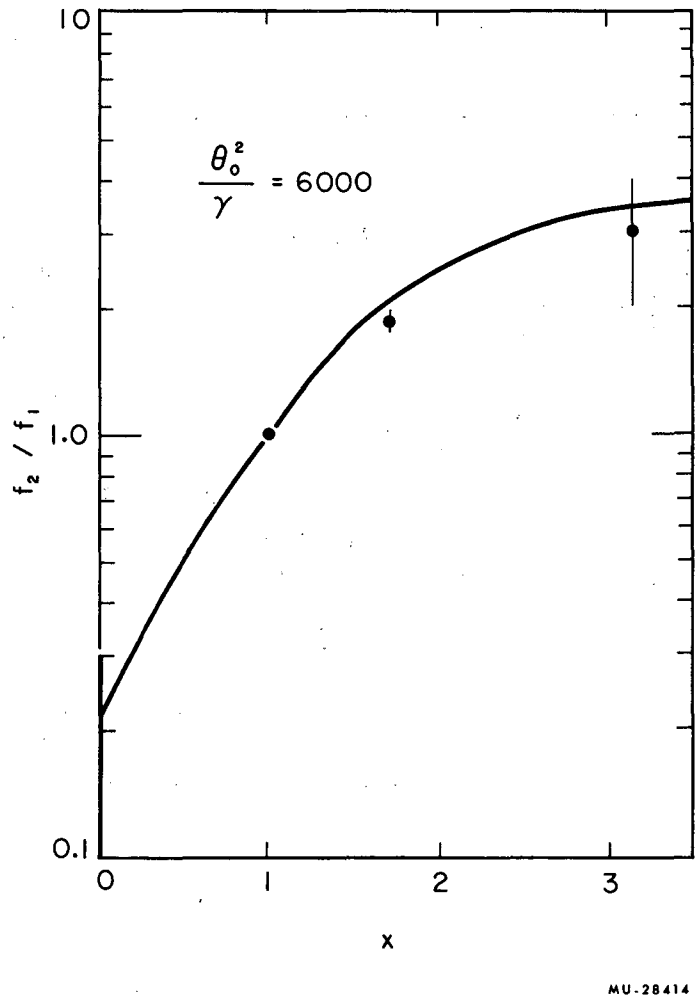

Fig. 6. Experimental and theoretical recoil-free fraction ratios. The parameter x is proportional to pressure. The solid curve was calculated for $\theta_o^2/\gamma = 6000$.

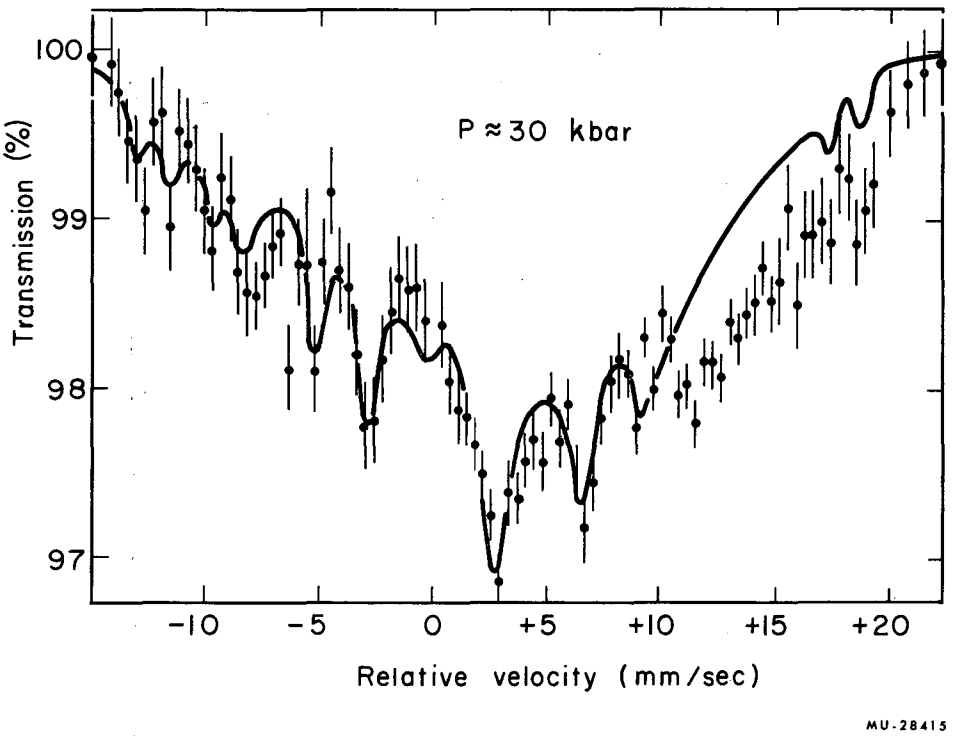

Fig. 7. Comparison of the experimental velocity spectrum at 30 kbar with a theoretical spectrum calculated by assuming pure quadrupole splitting in the source, with $\rho = -1.30$, and a narrow doublet pattern for the absorber.

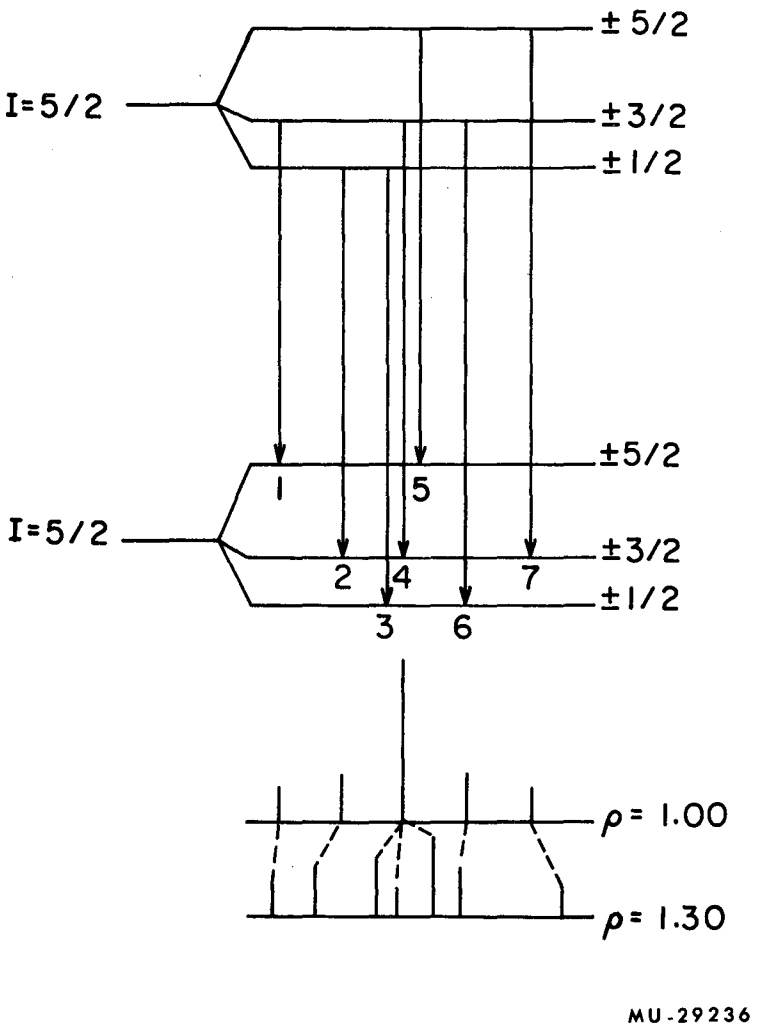

Fig. 8. Gamma-ray components between two nuclear levels, each with I = 5/2 and with pure electric quadrupole splitting. At the bottom, on energy scales, are the emission patterns associated with ρ = 1.00 and ρ = 1.30.